



Motion synchronization for semi-autonomous robotic swarm with a passivity-short human operator

Made Widhi Surya Atman¹ · Takeshi Hatanaka² · Zhihua Qu³ · Nikhil Chopra⁴ · Junya Yamauchi¹ · Masayuki Fujita¹

Received: 15 October 2017 / Accepted: 27 March 2018
© Springer Nature Singapore Pte Ltd. 2018

Abstract

This paper investigates coordination between a human operator and robotic swarm. The objective is to guarantee human-enabled motion synchronization to desired position/velocity references. The presence of a human in the system could improve performance in completing complex missions and adaptation to changes in environment or mission goal. Although in some works the human is modeled or assumed as a passive system, this does not always hold and a systematic solution to deal with non-passive humans is still needed. To this end, this paper assumes the human operator's process as a passivity-short system. Based on the positive feedback interconnection of passivity-short systems, we present a novel distributed control architecture interconnecting the human operator and the robotic swarm. The control goals are then proved to be achieved even in the presence of passivity shortage in the human operator. We finally demonstrate the proposed architecture through simulation studies and also implementation on an experimental testbed.

Keywords Semi-autonomous robotic swarm · Distributed motion synchronization · Interconnected passivity-short systems

1 Introduction

Distributed control of networked robotic swarms is expected to provide solutions to a wide range of applications such as environmental monitoring, infrastructure support or exploration due to its scalability and robustness against robot failures. Even though the robotic swarm is mostly expected to operate autonomously, mediacy of a human can be still beneficial or even necessary for completing complex missions over highly uncertain environment. Human's abilities

in perception and decision making could mitigate shortcomings in autonomy and adapt to changes in the environment or mission goal (Egerstedt 2014). Based on this perspective, cooperation control of semi-autonomous robotic swarm has been actively studied in recent years. Please refer to Wang and Zhang (2017), Kolling et al. (2016) and Music and Hirche (2017) for the state-of-the-art of this research field.

The semi-autonomous robot control systems have been in-depth studied in the field of bilateral teleoperation. One of the most standard approaches in the field is the passivity-based one, wherein the human operator (and environment) is modeled as a passive component, and then the stability of the overall system including the operator is rigorously guaranteed (Hokayem and Spong 2006; Nuno et al. 2011; Hatanaka et al. 2015b; Hirche and Buss 2012). Originally envisioned and studied as a single-master–single-slave robot architecture, the problem of bilateral teleoperation has also been extended to the multiple slave architecture (Lee and Spong 2005; Liu and Chopra 2012; Rodriguez-Seda et al. 2010; Franchi et al. 2012a, b; Secchi et al. 2012; Giordano et al. 2013; Wang and Wang 2017; Lee et al. 2013). The papers (Lee and Spong 2005; Liu and Chopra 2012; Rodriguez-Seda et al. 2010) consider centralized control architectures where a robot needs access to all of the slave robots, while (Franchi et al. 2012a; Secchi et al. 2012) focus on

Electronic supplementary material The online version of this article (<https://doi.org/10.1007/s41315-018-0056-8>) contains supplementary material, which is available to authorized users.

✉ Made Widhi Surya Atman
atman.m.aa@m.titech.ac.jp

- ¹ Department of Systems and Control Engineering, School of Engineering, Tokyo Institute of Technology, Tokyo, Japan
- ² Division of Electrical, Electronic and Information Engineering, Graduate School of Engineering, Osaka University, Osaka, Japan
- ³ Department of Electrical Engineering and Computer Science, University of Central Florida, Orlando, FL, USA
- ⁴ Department of Mechanical Engineering, University of Maryland, College Park, MD, USA

cooperative tasks in distributed control architectures where a master robot has access only to a member of the slave robots. Additionally, Franchi et al. (2012b) and Giordano et al. (2013) present extensions to more complex networks with multiple-master–multiple-slave scenario.

The main objective in the bilateral teleoperation is to guarantee good tracking performance and transparency with the help of force feedback. However, these are not always the central issues in various studies of human–swarm interactions/collaborations (Egerstedt 2014; Wang and Zhang 2017; Kolling et al. 2016; Music and Hirche 2017). In particular, in the case of high-level human–robot interactions, a simpler kinematic model without the dimension of force has been taken and accordingly force feedback to the human has not been assumed. As a matter of fact, many studies on the human–swarm interactions consider only visual feedback (Cummings 2004; McLurkin et al. 2006; Mekdeci and Cummings 2009; Olsen and Wood 2004). To this end, the authors have incorporated passivity paradigm for the vision-based interaction of a human and a class of semi-autonomous robotic swarms in Hatanaka et al. (2015a, 2017a, b).

Despite a great deal of success with the passivity-based approach, the assumption on the human passivity has been questioned in the literature e.g. see Colgate (1994), Dyck et al. (2013) and Atashzar et al. (2017) for haptic-based human–robot interactions and McRuer (1980) for vision-based interactions. In particular, McRuer (1980) claims that a human could learn an inverse model of the robot dynamics and adapt his/her own behavior depending on the dynamics so as not to attain passivity but to stabilize the system. The same tendency is also observed in the experimental studies in Hatanaka et al. (2017b). This means that the human passivity may be violated depending on the robot dynamics. In addition, the human model proposed in McRuer (1980) includes reaction delays, which is clearly a factor that violates passivity. The same issue is also addressed in Xia et al. (2015). Despite the efforts to treat the human passivity shortage in the above works, they deal with the single-master–single-slave robot architecture, and few works have been devoted to the semi-autonomous robotic swarm.

This paper presents a novel systematic approach to distributed control of the semi-autonomous robotic swarm based on a relatively new concept of interconnected passivity-short systems presented in Qu (2012) and Qu and Simaan (2014). Following this concept, the human operator is assumed to be a passivity-short system. The other parts are formulated in the same way as Hatanaka et al. (2015a, 2017b), wherein the control goal is set to synchronization of robot positions or velocities to a reference value desired by the operator under a distributed communication structure not only among robots but also between the operator and robots. We then present a new control architecture interconnecting the human operator and the robotic swarm based on the positive feedback

interconnections of passivity-short systems presented in Qu (2012) and Qu and Simaan (2014). The control goals, position and velocity synchronization, are then rigorously proved. Furthermore, we present a model-based discussion with simulation results and implementation on an experimental testbed to show the validity of the proposed architecture.

The remainder of this paper is organized as follows. Section 2 briefly introduces the concept of passivity-short systems which is the main background of this paper. In Sect. 3, the intended scenario is explained together with the passivity-based architecture in Hatanaka et al. (2015a, 2017a, b) and the difficulties faced in the presence of the human passivity shortage. The novel control architecture is then proposed in Sect. 4, and convergence analysis for the new architecture is presented in Sect. 5. The model-based verification of the human passivity shortage is discussed in Sect. 6 together with simulation results to verify the convergence. Finally, demonstration of the proposed architecture in an experimental testbed is presented in Sect. 7.

2 Preliminaries

This section is intended to introduce the concepts of passivity and passivity shortage which play central roles in this paper.

Definition 1 (Hatanaka et al. 2015b; Qu and Simaan 2014) The system $H : \mathcal{U} \rightarrow \mathcal{Y}$ with input $u \in \mathcal{U}$ and output $y \in \mathcal{Y}$ is said to be passive if there exists a constant $\beta \geq 0$ such that

$$\int_0^\tau y^T(t)u(t)dt \geq -\beta \quad (1)$$

for all input signals $u \in \mathcal{U}$ and for all $\tau \geq 0$. Moreover, the system is said to be (input feed-forward) passivity-short if there exists $\epsilon \geq 0$ such that

$$\int_0^\tau y^T(t)u(t)dt \geq -\beta - \epsilon \int_0^\tau \|u(t)\|^2 dt \quad (2)$$

for all input signals $u \in \mathcal{U}$ and for all $\tau \geq 0$, where ϵ is called impact coefficient.

From (1) and (2), passive systems are considered as a special case of passivity-short systems. Although passivity is preserved for the negative feedback interconnection of passive systems, a similar property is not guaranteed for passivity-short systems. However, it is shown in Qu and Simaan (2014) that stability may be ensured for positive-feedback interconnections of passivity-short systems with negative output self-feedbacks as shown in Fig. 1. In addition, this interconnection is also known to ensure output synchronization for the two passivity-short systems.

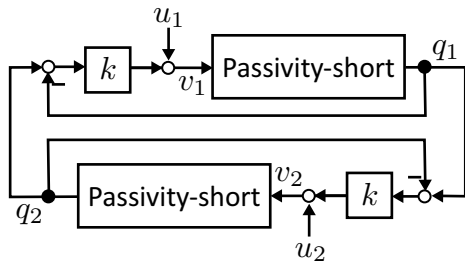


Fig. 1 Positive feedback interconnection of passivity-short systems

3 Human-enabled motion synchronization

In this section, we introduce the intended scenario of the human-enabled motion synchronization. Furthermore, we review the architecture designed in Hatanaka et al. (2015a, 2017b) based on passivity interconnection and clarify its problem on the human passivity shortage.

3.1 Intended scenario and objectives

Let us first introduce the intended scenario, as illustrated in Fig. 2. We consider interaction between a human operator and robotic swarm via a media interface. The human receives visual information on the robotic swarm and determines/sends a velocity command through the interface to the robots. The intended objective is for all robots to follow the human operator’s desired maneuvers.

In detail, the robotic swarm consists of n mobile robots $\mathcal{V} = \{1, \dots, n\}$ located on 2-D plane. All robots are connected to each other through a network to exchange information. The communication network is modeled as an undirected graph $G = (\mathcal{V}, \mathcal{E}), \mathcal{E} \subset \mathcal{V} \times \mathcal{V}$. Each robot i has

access to information of other neighboring robots belonging to the set $\mathcal{N}_i = \{j \in \mathcal{V} | (i, j) \in \mathcal{E}\}$. In addition, we have the following assumption.

Assumption 1 Graph G is fixed and connected.

Each robot’s dynamics is modeled as a single integrator, described as

$$\dot{q}_i = u_i, \quad i \in \mathcal{V} \tag{3}$$

with $q_i \in \mathbb{R}^2$ and $u_i \in \mathbb{R}^2$ denoting position and velocity input of each robot i , respectively. To ease the implementation, robots accessible from the human are restricted to a subset $\mathcal{V}_h \subseteq \mathcal{V}$. Namely, robots only in \mathcal{V}_h are affected by the human’s input and the operator gains information only on \mathcal{V}_h . In the sequel, we use the notation δ_i such that $\delta_i = 1$ for $i \in \mathcal{V}_h$ or 0 otherwise.

In this paper, we consider two fundamental goals which are position and velocity control. The position control goal is defined as

$$\lim_{t \rightarrow \infty} \|q_i - r_q\| = 0, \quad \forall i \in \mathcal{V}, \tag{4}$$

where all of the robots asymptotically approach the position reference r_q . The velocity control goal is defined as

$$\lim_{t \rightarrow \infty} \|\dot{q}_i - r_v\| = 0, \quad \lim_{t \rightarrow \infty} \|q_i - q_j\| = 0, \quad \forall i, j \in \mathcal{V}, \tag{5}$$

which means that all robots follow the desired velocity reference r_v while their position converges. Either of these control goals, called position control mode and velocity control mode respectively, is selected by the operator. In addition, references r_q and r_v are assumed to exist only in the human operator’s brain, and these values are unknown to robots. The control objective is to design an architecture to fulfill

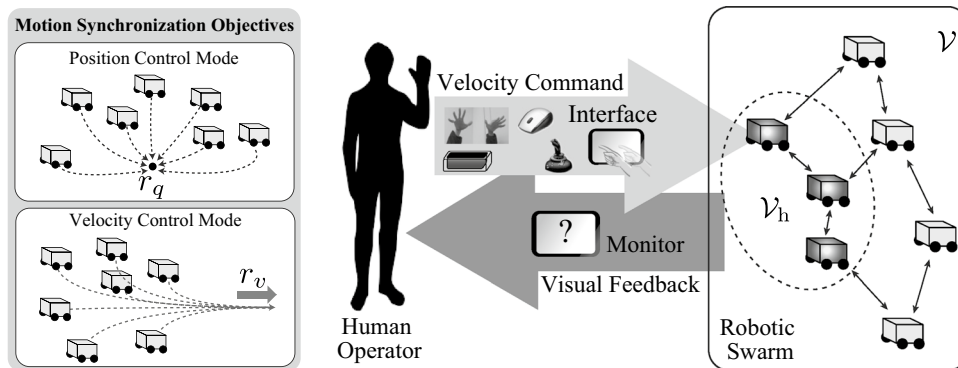


Fig. 2 Illustration for the intended scenario where a human operator interacts with a set of accessible robots \mathcal{V}_h by sending a velocity command through an interface and receiving visual feedback from a monitor. Through two different control modes, all robots converge

to the human’s desired position r_q (position control mode) or move together with the same velocity as human’s desired velocity r_v (velocity control mode)

the above two fundamental goals (4) and (5) depending on the selected control mode.

Remark 1 Dynamics of a standard wheeled robot with non-holonomic constraints is known to be reduced to (3) by using the so-called look ahead control together with input-output feedback linearization in Yun and Yamamoto (1993). In addition, our intended scenario considers high-level control problem and hence we focus on the low frequency domain, wherein the dynamics is expected to be modeled by (3).

Remark 2 The two goals in (4) and (5) represent the problems in navigating the robotic swarm on 2-D plane. As position control mode is used to navigate them to a certain position, the velocity control mode can be utilized in a long distance navigation where the velocity is considered as another important control objective.

Remark 3 Although (4) and (5) imply collisions among robots, adding biases to the actual robot positions and regarding each q_i as a virtual position would trivially avoid collisions at least in the final configuration. While it is important to consider collision avoidance in transient state as in Stipanovic et al. (2007), it tends to make the robotic swarm’s dynamics and human behavior too complicated to apply the human model from McRuer (1980) and the model-based design which is the main focus of this paper. Therefore, in this specific paper, we consider this simpler formulation with bias. Collision avoidance in the transient state is left as a future work.

3.2 Passivity-based architecture

In this subsection, we introduce the passivity-based control architecture presented in Hatanaka et al. (2015a, 2017b). In the system, the velocity input u_i is designed based on PI consensus algorithm (Freeman et al. 2006; Bai et al. 2010) as

$$u_i = \delta_i u_h + \sum_{j \in \mathcal{N}_i} a_{ij}(q_j - q_i) + \sum_{j \in \mathcal{N}_i} b_{ij}(\xi_i - \xi_j) \tag{6a}$$

$$\dot{\xi}_i = \sum_{j \in \mathcal{N}_i} b_{ij}(q_j - q_i), \tag{6b}$$

where $u_h \in \mathbb{R}^2$ is the command which is sent from the operator and $\xi_i \in \mathbb{R}^2$ denotes the internal state of each robot. The gains $a_{ij} = a_{ji} \forall i, j \in \mathcal{V}$, $a_{ij} > 0$ if $(i, j) \in \mathcal{E}$, and $a_{ij} = 0$ otherwise, and b_{ij} also obey the same rule.

Combining (3) and (6), and defining $q = [q_1^T \dots q_n^T]^T$, $\xi = [\xi_1^T \dots \xi_n^T]^T$, the collective robots dynamics could be represented as

$$\begin{bmatrix} \dot{q} \\ \dot{\xi} \end{bmatrix} = \begin{bmatrix} -\bar{L}_p & \bar{L}_l \\ -\bar{L}_l & 0 \end{bmatrix} \begin{bmatrix} q \\ \xi \end{bmatrix} + \begin{bmatrix} D \otimes I_2 \\ 0 \end{bmatrix} u_h, \tag{7}$$

with matrix $D := [\delta_1 \dots \delta_n]^T$, $\bar{L}_p := L_p \otimes I_2$ and $\bar{L}_l := L_l \otimes I_2$. The symbol \otimes describes the Kronecker product, while L_p and L_l denote the $n \times n$ graph Laplacian associated with the adjacency matrix for element a_{ij} and b_{ij} , respectively.

Let us define the average position of accessible robots as

$$z_q = \frac{1}{m}(D \otimes I_2)^T q, \tag{8}$$

with m as the number of elements in \mathcal{V}_h . Then, passivity of the robotic swarm could be stated by the following lemma.

Lemma 1 (Hatanaka et al. 2017b) *Under Assumption 1, the system (7) describing the robotic swarm is passive from u_h to z_q with respect to the storage function*

$$S^q = \frac{1}{2m} \|q\|^2 + \frac{1}{2m} \|\xi\|^2 \geq 0. \tag{9}$$

In the velocity control mode, let us consider virtually rewritten dynamics of the robotic network by assuming differentiability of u_h .¹ Considering \dot{u}_h as input of the system, the dynamic is rewritten as

$$\begin{bmatrix} \ddot{q} \\ \ddot{\xi} \\ \dot{q} \\ \dot{\xi} \\ \dot{u}_h \end{bmatrix} = \begin{bmatrix} -\bar{L}_p & \bar{L}_l \\ -\bar{L}_l & 0 \\ I_{2n} & 0 \\ 0 & I_{2n} \\ 0 & 0 \end{bmatrix} \begin{bmatrix} \dot{q} \\ \dot{\xi} \\ q \\ \xi \\ u_h \end{bmatrix} + \begin{bmatrix} D \otimes I_2 \\ 0 \\ 0 \\ 0 \\ I_2 \end{bmatrix} \dot{u}_h, \tag{10}$$

where O is the $(8n + 2) \times (4n + 2)$ zero matrix.

In the same way as the position control, defining the average velocity of accessible robots as

$$z_v = \frac{1}{m}(D \otimes I_2)^T \dot{q} \tag{11}$$

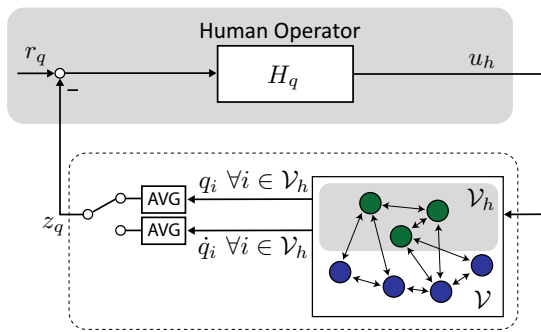
we can state passivity as the following lemma.

Lemma 2 (Hatanaka et al. 2017b) *Under Assumption 1, the system (10) describing the robotic network is passive from \dot{u}_h to z_v with respect to the storage function*

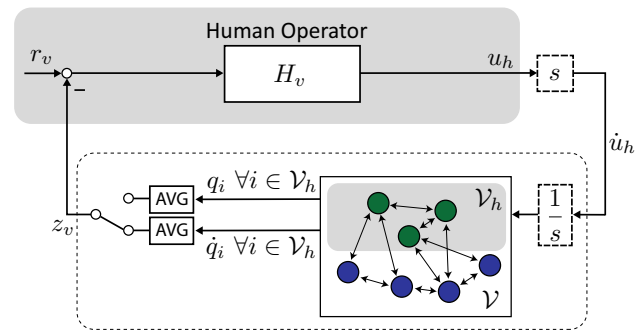
$$S^v = \frac{1}{2m} \|\dot{q}\|^2 + \frac{1}{2m} \|\dot{\xi}\|^2 \geq 0. \tag{12}$$

The above two lemmas together with the well-known energy dissipation property for the feedback interconnection of passive systems (Hatanaka et al. 2015b) motivates us to present the architectures in Fig. 3a, b under the

¹ Differentiability of u_h is guaranteed by inserting a filter just after the human operator block. See Hatanaka et al. (2015a, 2017b) for more details on this issue.



(a) Block diagram of the passivity-based architecture for position control mode



(b) Block diagram of the passivity-based architecture for velocity control mode with virtual differential/integral

Fig. 3 Passivity-based architecture for position and velocity control mode. In the position control mode, the human operator compares the desired position r_q with the average position z_q of the accessible robots. While in the velocity control mode, the human operator compares

the desired velocity r_v with the average velocity z_v of the accessible robots. In both control modes, the human sends a velocity command u_h

hypothesis that the operator's blocks H_q and H_v are passive. Furthermore, the goals (4) and (5) are proved to be achieved under the human passivity assumption together with several reasonable assumptions. Readers are suggested to refer to Hatanaka et al. (2015a, 2017b) for further details.

3.3 What if an operator is passivity-short?

As mentioned in Sect. 1, the assumption on human passivity has been questioned in the literature. Among them, we mainly focus on McRuer (1980) which treats a vision-based interaction between an operator and robot similar to this paper. The authors in McRuer (1980) present a human operator model $H(s)$ formulated as

$$H(s)T(s) = \frac{\omega_c}{s} e^{-\tau s}, \quad (13)$$

where $T(s)$ is the transfer function describing the robot dynamics, ω_c is the gain crossover frequency and τ is the processing delay in the brain. The model implies that the operator learns an inverse model of the robot dynamics $T(s)$ and behaves so as to cancel $T(s)$ and that the gain diagram of the open-loop transfer function $H(s)T(s)$ has the same slope as the single integrator. The same tendency is also observed for the passivity-based system as shown in the section on the human modeling in Hatanaka et al. (2015a, 2017b). This means that, even if the processing delay is ignored, the human operator can violate passivity e.g. when the phase of $T(s)$ exceeds 90deg. It is easy to confirm that this happens when the inter-robot network is sparse as mentioned in Hatanaka et al. (2015a). More importantly, in the presence of the delay τ , human passivity can no longer be expected.

It is also observed in Hatanaka et al. (2015a, 2017b) that human passivity can be lost when the operator is not sufficiently trained, even if the phase of $T(s)$ does not exceed

90deg and the delay is ignorably small relative to the focused frequency domain. Studies in Hatanaka et al. (2015a, 2017b) experimentally demonstrate that trainings have positive effects on human passivity but an architecture assuming skillful operators is not always realistic. In this sense, it is important to establish a control architecture achieving control goals even in the presence of the human passivity shortage.

In order to expand the class of the operators, we take the concept of the passivity shortage in Definition 1. Suppose now that the operator is passivity-short with impact coefficient ϵ under the same architecture as in the previous subsection. For brevity, we consider only the position control problem with $r_q = 0$. In this case, under the above mentioned assumption of the passivity-short human, there must exist $\beta \geq 0$ such that

$$\int_0^\tau u_h(t)^T (-z_q(t)) dt > -\beta - \epsilon \int_0^\tau \|z_q(t)\|^2 dt.$$

In other words, defining

$$S^h = \int_0^\tau u_h(t)^T (-z_q(t)) dt + \epsilon \int_0^\tau \|z_q(t)\|^2 dt + \beta,$$

it is always nonnegative. Then, following the same procedure as Hatanaka et al. (2015a), the time derivative of the total energy $S^q + S^h$ along the system trajectories is given by

$$\dot{S}^q + \dot{S}^h = -\frac{1}{m} q^T \bar{L}_p q + z_q^T u_h - z_q^T u_h + \epsilon \|z_q\|^2 \quad (14)$$

$$= -\frac{1}{m} q^T \bar{L}_p q + \epsilon \|z_q\|^2. \quad (15)$$

Here, the energy function is guaranteed to be decreasing only when $\epsilon = 0$, namely when the human is passive. Conversely, when $\epsilon > 0$, it is not difficult to confirm that the nonnegative second term in (15) cannot be canceled out by

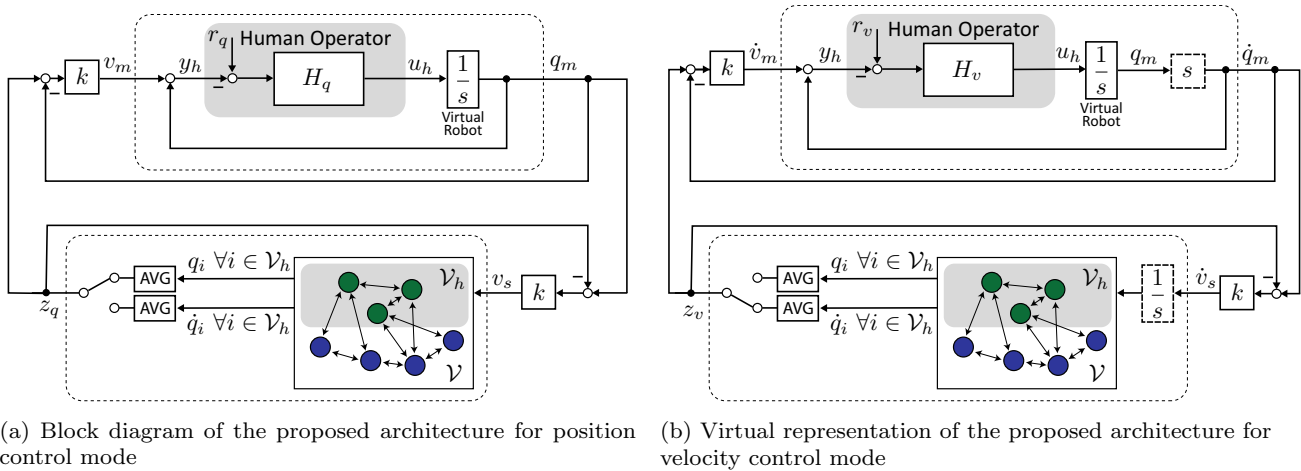


Fig. 4 Proposed control architecture for position and velocity control mode using the concept of interconnection of passivity-short systems. The human operator now sends the velocity command u_h to the vir-

tual master robot instead of sending it directly to the robotic swarm. The visual feedback y_h is then designed to ensure that the goals in (4) or (5) is achieved when $y_h = r_q$ or $y_h = r_v$, respectively

the nonpositive first term in (15) by just changing control parameters like a_{ij} in L_p . Thus, the energy dissipation is not trivially proved for the system architecture in Fig. 3a even if ϵ is small.

4 Proposed control architecture

In this section, we present novel architectures for both position and velocity control mode based on the concept of interconnected passivity-short systems in Fig. 1

4.1 Architecture for position control mode

We start with considering the position control mode. The basic idea is to regard the robotic swarm and the operator as two passivity-short systems in Fig. 1.

Based on the fact that Fig. 1 achieves output synchronization, we need to ensure that:

- the outputs of the robotic swarm and human operator must be physical quantities with a common dimension, e.g. position-position or velocity-velocity.

Regarding this issue, it is easily confirmed in Fig. 3a that the output of the operator is a quantity with dimension equal to velocity, while that of the robotic swarm has a dimension equal to position. To eliminate the mismatch, we place a virtual robot in the operator side and u_h is added to it instead of the actual

robots as illustrated in Fig. 4a. In this paper, for simplicity, we take the single integrator model

$$\dot{q}_m = u_h \tag{16}$$

as the dynamics of the virtual robot. We then let the virtual robot send its own position, denoted by q_m , as the output of the human operator side. Under this modification, the outputs in Fig. 1 are given by $q_1 = q_m$ and $q_2 = z_q$, and hence both have dimension of position.

Meanwhile, the human behaves so as to drive visual feedback information, denoted by y_h , to the reference r_q . Accordingly, when $y_h = r_q$, the operator would stop sending a command, namely $u_h = 0$. In this case, it is expected that the control goal (4) is satisfied. Assuming that position synchronization will be eventually achieved among $q_i, i \in \mathcal{V}$ and q_m , the requirement is described as below:

$$- y_h = r_q \text{ with } q_i = q_j \forall i, j \in \mathcal{V} \cup \{m\} \Rightarrow (4).$$

It is easy to confirm that, just following the architecture of Fig. 1, the input to the human, v_1 in Fig. 1, is equal to $v_1 = k(z_q - q_m)$, which can be zero even if (4) is not satisfied. To eliminate the problem, we add a local feedback path which results in

$$y_h = q_m + k(z_q - q_m) = kz_q + (1 - k)q_m. \tag{17}$$

Namely, as long as k is selected as $k \in (0, 1)$, the information y_h becomes equal to the weighted average of $q_i, i \in \mathcal{V}$ and q_m . Under this modification, it is ensured that $y_h = r_q$ and

$q_i = q_j \forall i, j \in \mathcal{V} \cup \{m\}$ means (4). In summary, we consider the architecture in Fig. 4a.

Let us next examine if both of the operator and robotic swarm are passivity-short. The robotic swarm encircled by the dashed line is the same as that in Fig. 3a and hence the system formulated as

$$\begin{bmatrix} \dot{q} \\ \dot{\xi} \end{bmatrix} = \begin{bmatrix} -\bar{L}_p & \bar{L}_l \\ -\bar{L}_l & 0 \end{bmatrix} \begin{bmatrix} q \\ \xi \end{bmatrix} + \begin{bmatrix} D \otimes I_2 \\ 0 \end{bmatrix} v_s, \quad (18)$$

is passive, in other words, passivity-short with $\epsilon = 0$ as formally stated below.

Corollary 1 Under Assumption 1, the system (18) is passivity-short with $\epsilon = 0$ from v_s to z_q with respect to the storage function S^q .

We next investigate the passivity-short property of the human operator. In this paper, we assume the following properties on the human.

Assumption 2

- r_q is constant.
- Combination of human and virtual master robot is input passivity-short from $r_q - y_h$ to $q_m - r_q$ with $\exists \epsilon \in (0, 1)$, i.e., $\exists \beta \geq 0$ such that

$$\begin{aligned} \int_0^\tau (q_m(t) - r_q)^T (r_q - y_h(t)) dt \\ \geq -\beta - \epsilon \int_0^\tau \|r_q - y_h(t)\|^2 dt. \end{aligned}$$

Remark that we assume passivity-shortage of not the human block H_q but the cascade system of H_q and the integrator just after H_q in Fig. 4a, whose validity will be examined in Sect. 6.

Let us now define $\bar{q}_m = q_m - r_q$. We then have the following lemma.

Lemma 3 Under Assumption 2, the system describing the human and virtual master robot is passivity-short from v_m to \bar{q}_m with impact coefficient 1 with respect to the storage function

$$\begin{aligned} S_m^q &= \int_0^\tau (q_m(t) - r_q)^T (r_q - y_h(t)) dt \\ &+ \epsilon \int_0^\tau \|r_q - y_h(t)\|^2 dt + \beta. \end{aligned}$$

Proof Taking the time derivative of the storage function S_m and using the definition of y_h and \bar{q}_m , we have

$$\begin{aligned} \dot{S}_m^q &= \bar{q}_m^T (-v_m - \bar{q}_m) + \epsilon \|v_m + \bar{q}_m\|^2 \\ &= (-1 + 2\epsilon) \bar{q}_m^T v_m + \epsilon \|v_m\|^2 + (-1 + \epsilon) \|\bar{q}_m\|^2 \\ &= \bar{q}_m^T v_m + \|v_m\|^2 - (1 - \epsilon) \|v_m + \bar{q}_m\|^2 \\ &\leq \bar{q}_m^T v_m + \|v_m\|^2. \end{aligned} \quad (19)$$

This completes the proof. \square

4.2 Architecture for velocity control mode

We continue with the architecture for velocity control. Also in this case, to eliminate the mismatch of the outputs between the operator and robotic swarm, we place a virtual robot. The variables to be synchronized should be changed from positions to velocities according to the change of the objective. We thus let the operator and robotic swarm exchange velocity \dot{q}_m and average velocity z_v . We also determine the visual feedback information y_h by the derivative of (17) as

$$y_h = kz_v + (1 - k)\dot{q}_m. \quad (20)$$

The entire system is then illustrated in Fig. 4b.

Similarly to the position control mode, the robotic swarm encircled by the dashed line in Fig. 4b formulated as

$$\begin{bmatrix} \ddot{q} \\ \ddot{\xi} \\ \dot{q} \\ \dot{\xi} \\ \dot{v}_s \end{bmatrix} = \begin{bmatrix} -\bar{L}_p & \bar{L}_l \\ -\bar{L}_l & 0 \\ I_{2n} & 0 \\ 0 & I_{2n} \\ 0 & 0 \end{bmatrix} \begin{bmatrix} \dot{q} \\ \dot{\xi} \\ q \\ \xi \\ v_s \end{bmatrix} + \begin{bmatrix} D \otimes I_2 \\ 0 \\ 0 \\ 0 \\ I_2 \end{bmatrix} \dot{v}_s \quad (21)$$

is the same as that in Fig. 3b. We thus obtain the following corollary in the same way as Lemma 2.

Corollary 2 Under Assumption 1, the system (18) describing the robotic network is passive and hence passivity-short with $\epsilon = 0$ from \dot{v}_s to z_v with respect to the storage function S^v .

Let us now assume the following assumption compatible with Assumption 2.

Assumption 3

- r_v is constant.
- Human is input passivity-short from $r_v - y_h$ to $\dot{q}_m - r_v$ with impact coefficient $\epsilon \in (0, 1)$, i.e., $\exists \beta \geq 0$ such that

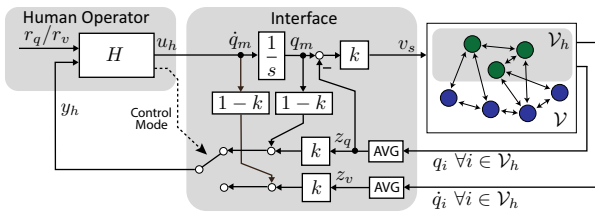


Fig. 5 Combination architecture for both position and velocity control mode

$$\int_0^\tau (\dot{q}_m(t) - r_v)^T (r_v - y_h(t)) dt \geq -\beta - \epsilon \int_0^\tau \|r_v - y_h(t)\|^2 dt.$$

Define $\check{q}_m = q_m - \int_0^\tau r_v dt$. Then, similarly to Lemma 3, the following lemma is proved.

Lemma 4 Under Assumption 3, the system describing the human and virtual master robot is passivity-short with impact coefficient 1 from \dot{v}_m to \check{q}_m with respect to the storage function

$$S_m^v = \int_0^\tau (\dot{q}_m(t) - r_v)^T (r_v - y_h(t)) dt + \epsilon \int_0^\tau \|r_v - y_h(t)\|^2 dt + \beta$$

Proof We show the proof by taking the time derivative of the storage function S_m^v

$$\begin{aligned} \dot{S}_m^v &= \check{q}_m^T (-\dot{v}_m - \dot{\check{q}}_m) + \epsilon \|\dot{v}_m + \dot{\check{q}}_m\|^2 \\ &= \check{q}_m^T \dot{v}_m + \|\dot{v}_m\|^2 - (1 - \epsilon) \|\dot{v}_m + \dot{\check{q}}_m\|^2 \\ &\leq \check{q}_m^T \dot{v}_m + \|\dot{v}_m\|^2. \end{aligned} \tag{22}$$

This completes the proof. □

4.3 Combination of position and velocity control modes

Fig. 4a, b are useful for analyzing stability and synchronization but they are not directly implementable since the averaging block and the feedback path from z_q to v_s or z_v to \dot{v}_s is not executable under distributed information exchanges among robots. We thus equivalently transform the combination of Figs. 4a, b to 5. In the figure, the operations in the middle block are assumed to be executed in the interface placed in the human side, which is implementable even under communication constraints. Then, both of the leftmost block (human operator) and

rightmost block (robotic swarm) is essentially the same as the passivity-based architecture in Hatanaka et al. (2015a, 2017b). The only difference is in the middle block, which allows one to achieve the control goals even in the presence of passivity shortage in the human as proved in the next section.

5 Convergence analysis

In this section, we present the convergence analysis to show that the synchronization goals in (4) and (5) are guaranteed for the proposed architectures.

5.1 Synchronization in position control mode

In this subsection, we prove the goal (4) in the position control mode. We start with introducing additional assumptions regarding boundedness of the signals.

Assumption 4

- The position of the virtual master robot q_m is bounded.
- If input $r_q - y_h$ to the human is bounded, then output u_h of the human block is also bounded.

Both assumptions look reasonable in practice. Then, we present our results for position control mode.

Theorem 1 Consider the interconnected system in Fig. 4a with $k \in (0, 1)$ consisting of the robotic network (7) satisfying Assumption 1 and a human operator satisfying Assumptions 2 and 4. Then, the system achieves the control goal (4).

Proof Defining $\bar{q} = q - (\mathbf{1}_n \otimes I_2)r_q$, we could reformulate the dynamics of the robotic swarm as

$$\dot{\bar{q}} = -\bar{L}_P \bar{q} + \bar{L}_I \xi + (D \otimes I_2)v_s, \tag{23a}$$

$$\dot{\xi} = -\bar{L}_I \bar{q}, \tag{23b}$$

$$\bar{z}_q = \frac{1}{m} (D \otimes I_2)^T \bar{q}, \tag{23c}$$

which is also passive from v_s to \bar{z}_q with respect to the storage function $S_s^q = \frac{1}{2m} \|\bar{q}\|^2 + \frac{1}{2m} \|\xi\|^2 > 0$. To be precise, we can derive

$$\dot{S}_s^q = -\frac{1}{m} \bar{q}^T \bar{L}_P \bar{q} + \bar{z}_q^T v_s \leq \bar{z}_q^T v_s. \tag{24}$$

Let us now define $V_q = S_m^q + S_s^q$. Then, the time derivative of V_q along the system trajectories is given as

$$\begin{aligned} \dot{V}_q &= \tilde{q}_m^T k(\tilde{z}_q - \tilde{q}_m) + k^2 \|\tilde{z}_q - \tilde{q}_m\|^2 - \frac{1}{m} \tilde{q}^T \bar{L}_P \tilde{q} \\ &\quad - (1 - \epsilon) \|v_m + \tilde{q}_m\|^2 + \tilde{z}_q^T k(\tilde{q}_m - \tilde{z}_q) \\ &= -k(1 - k) \|\tilde{z}_q - \tilde{q}_m\|^2 - \frac{1}{m} \tilde{q}^T \bar{L}_P \tilde{q} \\ &\quad - (1 - \epsilon) \|v_m + \tilde{q}_m\|^2. \end{aligned}$$

Since $\dot{V}_q \leq 0$ holds if $k \in (0, 1)$, which means boundedness of q , ξ and z_q from the definition of S_s^q . Then, since $\dot{\xi} = -\bar{L}_P q$, ξ is also bounded. Boundedness of z_q and q_m from Assumption 4 means that v_m and v_s are also bounded. From $\dot{q} = -\bar{L}_P q + \bar{L}_I \xi + (D \otimes I_2) v_s$, \dot{q} is also proved to be bounded. Next, since $r - y_h$ is bounded, then by Assumption 4, the human command $u_h = \dot{q}_m$ is also bounded. In addition, by using boundedness of \dot{q}_m and \dot{z}_q we can state boundedness of \dot{v}_m and \dot{v}_s . In summary, invoking Barbalat's Lemma, we have $\lim_{t \rightarrow \infty} \|z_q - q_m\| = 0$, $\lim_{t \rightarrow \infty} \tilde{q}^T \bar{L}_P \tilde{q} = 0$, and $\lim_{t \rightarrow \infty} \|\tilde{q}_m + v_m\| = 0$.

The term $\lim_{t \rightarrow \infty} \tilde{q}^T \bar{L}_P \tilde{q} = 0$ implies position synchronization, i.e., $\exists c(\cdot)$ such that $q_i(t) - c(t) \rightarrow 0 \forall i \in \mathcal{V}$. Then, we also have $z_q(t) - c(t) \rightarrow 0$. In addition, the term $\lim_{t \rightarrow \infty} \|z_q - q_m\| = 0$ means that $q_m(t) - c(t) \rightarrow 0$, which also implies $v_m(t) \rightarrow 0$ and $v_s(t) \rightarrow 0$. Combining $v_m(t) \rightarrow 0$ and $\lim_{t \rightarrow \infty} \|\tilde{q}_m + v_m\| = 0$, we also obtain $\tilde{q}_m(t) \rightarrow 0$, which means that $q_m(t) \rightarrow r_q$ and hence $c(t) \rightarrow r_q$. We thus can conclude $\lim_{t \rightarrow \infty} \|q_i - r_q\| = 0$ for all $i \in \mathcal{V}$. \square

5.2 Synchronization in velocity control mode

We next consider the velocity control mode. Let us add the following assumption.

Assumption 5 The human operator block is time invariant and there exists a time-invariant storage function such that

$$\dot{S}_m^v \leq (\dot{q}_m(t) - r_v)^T (r_v - y_h(t)) + \epsilon \|r_v - y_h(t)\|^2$$

with ϵ in Assumption 3. In addition, if input to the human $r_v - y_h$ is bounded, the internal states and output u_h of the human block are also bounded.

Then, we can state the main result for velocity control.

Theorem 2 Consider the interconnected system in Fig. 4b with $k \in (0, 1)$ consisting of the robotic network (10) satisfying Assumption 1 and a human operator satisfying Assumptions 3 and 5. Then, the system achieves the control goal (5).

Proof Define $\tilde{q} = q - (\mathbf{1}_n \otimes I_2)(\int_0^t r_v d\tau)$ and $\tilde{\xi} = \bar{L}_I \xi$. Then, we could represent the dynamics of the robotic swarm as

$$\dot{\tilde{q}} = -\bar{L}_P \tilde{q} + \tilde{\xi} + (D \otimes I_2) v_s - (\mathbf{1}_n \otimes I_2) r_v, \quad (25a)$$

$$\dot{\tilde{\xi}} = -\bar{L}_I^2 \tilde{q}, \quad (25b)$$

$$\tilde{z}_v = \frac{1}{m} (D \otimes I_2)^T \dot{\tilde{q}}, \quad (25c)$$

which is also passive from \dot{v}_s to \tilde{z}_v with regards to the storage function $S_s^v = \frac{1}{2m} \|\dot{\tilde{q}}\|^2 + \frac{1}{2m} \tilde{q}^T \bar{L}_I^2 \tilde{q} \geq 0$. Again, by taking the time derivative of S_s^v , we obtain

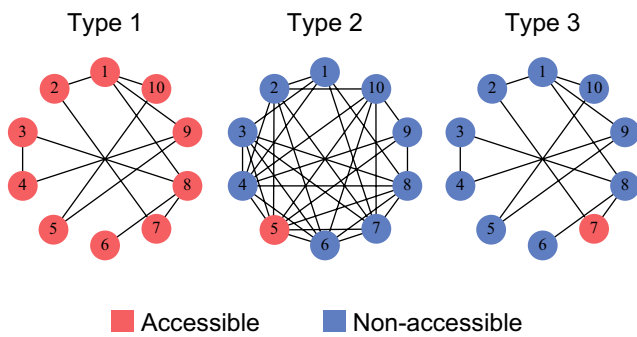
$$\begin{aligned} \dot{S}_s^v &= \frac{1}{m} \dot{\tilde{q}}^T (-\bar{L}_P \dot{\tilde{q}} - \bar{L}_I^2 \tilde{q} + (D \otimes I_2) \dot{v}_s) + \frac{1}{m} \tilde{q}^T \bar{L}_I^2 \dot{\tilde{q}} \\ &= -\frac{1}{m} \dot{\tilde{q}}^T \bar{L}_P \dot{\tilde{q}} + \tilde{z}_v^T \dot{v}_s \leq \tilde{z}_v^T \dot{v}_s. \end{aligned} \quad (26)$$

Therefore, defining $V_v = S_m^v + \tilde{S}_s^v$, we get

$$\begin{aligned} \dot{V}_v &= \tilde{q}_m^T k(\tilde{z}_v - \dot{\tilde{q}}_m) + k^2 \|\tilde{z}_v - \dot{\tilde{q}}_m\|^2 - \frac{1}{m} \dot{\tilde{q}}^T \bar{L}_P \dot{\tilde{q}} \\ &\quad - (1 - \epsilon) \|\dot{v}_m + \dot{\tilde{q}}_m\|^2 + \tilde{z}_v^T k(\dot{\tilde{q}}_m - \tilde{z}_v) \\ &= -k(1 - k) \|\tilde{z}_v - \dot{\tilde{q}}_m\|^2 - \frac{1}{m} \dot{\tilde{q}}^T \bar{L}_P \dot{\tilde{q}} \\ &\quad - (1 - \epsilon) \|\dot{v}_m + \dot{\tilde{q}}_m\|^2. \end{aligned}$$

Since $\dot{V}_v \leq 0$ under $k \in (0, 1)$, $\dot{\tilde{q}}$ and $\bar{L}_I \tilde{q}$ are proved to be bounded from the definition of \tilde{S}_s^v , which also means boundedness of \tilde{z}_v and $\tilde{\xi}$. Then, Assumption 5 implies that boundedness of $u_h = \dot{q}_m$ depends on boundedness of \dot{q}_m itself and z_v . We thus consider the boundedness of $\dot{\tilde{q}}_m$, which coincides with boundedness of \dot{v}_m and \dot{v}_s . In addition, by inspecting (25a) we can state that $\tilde{\xi}$ is bounded. Thus, there exists a positively invariant set for system (25a, 25b) and LaSalle's principle is applicable under Assumption 5.

Note that $\dot{V}_v = 0$ is equivalent to $\bar{L}_P \dot{\tilde{q}} = 0$, $z_v - \dot{\tilde{q}}_m = 0$ and $\dot{v}_m + \dot{\tilde{q}}_m = 0$. Considering the trajectories of the system identically satisfying the above conditions which imply that $\dot{v}_m(t) = 0$, $\dot{v}_s(t) = 0$ and velocity synchronization, i.e., $\exists v(\cdot)$ such that $\dot{q}_i(t) = v(t) \forall i \in \mathcal{V}$, hence $z_v(t) = v(t)$. Then, we also have $\dot{q}_m(t) = v(t)$. Combining $\dot{v}_m(t) + \dot{\tilde{q}}_m(t) = 0$ and $\dot{v}_m(t) = 0$, we also obtain $\dot{\tilde{q}}_m(t) = 0$, which means $\dot{q}_m(t) = r_v$ and hence $v(t) = r_v$. We thus confirm that $\dot{q}_i = r_v \forall i \in \mathcal{V}$. In addition, since the assumption of $\bar{L}_I \tilde{q} \neq 0$ contradicts boundedness of $\tilde{\xi}$ in (25b), we can conclude position synchronization. This completes the proof. \square



(a) Three graph types from [23]

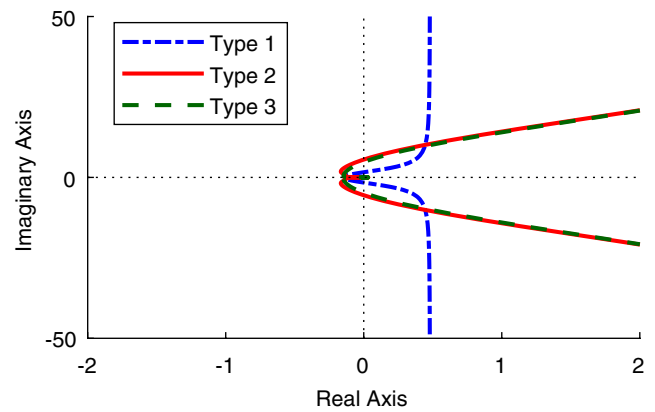
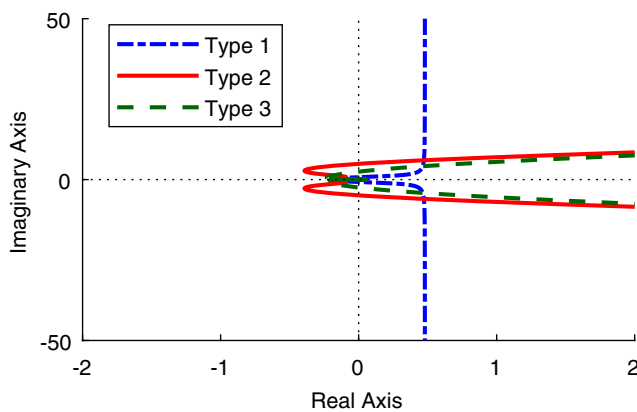
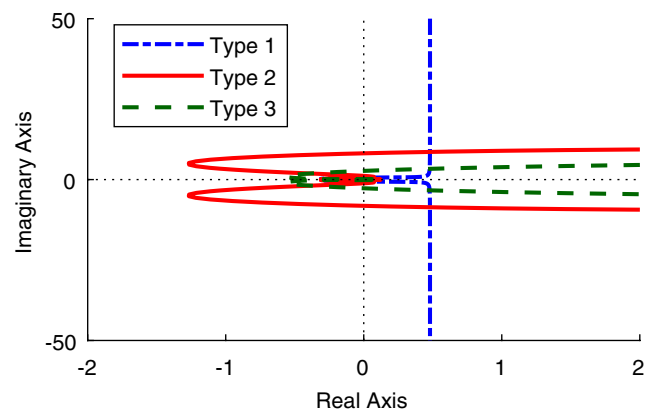
(b) Nyquist plot for $(1/s)H(s)$ with $k = 0.2$ (c) Nyquist plot for $(1/s)H(s)$ with $k = 0.5$ (d) Nyquist plot for $(1/s)H(s)$ with $k = 0.8$

Fig. 6 Nyquist plots for $(1/s)H(s)$ based on the model (13) with various k values for the three different types of networks. Here, only Type 2 with $k = 0.8$ violates the assumption that $\epsilon < 1$ (i.e. $\text{Re}[(1/s)H(s)] > -1$)

6 Model-based verification

In this section, we present a discussion regarding the passivity-short assumption on the human operator based on the model (13) from McRuer (1980). Furthermore, we present simulation results by using the transfer function of the human operator (13) to verify the goals in (4) and (5) are achieved.

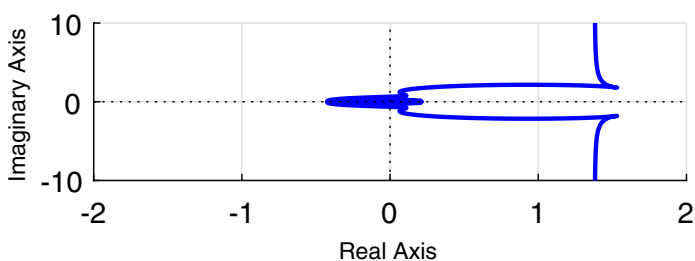
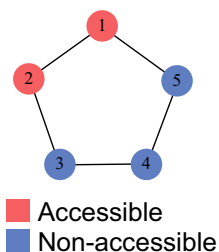
6.1 Verification on human passivity

In this subsection, we examine if modeling the operator with the virtual robot as a passivity-short system with $\epsilon \in (0, 1)$ is reasonable. It is now pointed out in Qu (2012) and Qu and Simaan (2014) that if the Nyquist plot of a SISO linear time-invariant and Lyapunov stable system (all poles are in the left-half space except for at most a single pole at the origin) lies within a domain with real part greater than $-\epsilon$, then the system is passivity-short with impact coefficient ϵ .

Based on the above fact, we take the model $H(s)$ in (13) as the human operator model and check the Nyquist plot of the cascade system $(1/s)H(s)$, where we take $\omega_c = 0.6 \text{ rad/s}$ based on the human model in Hatanaka et al. (2015a) and the same $\tau = 0.2 \text{ s}$ as McRuer (1980). In the new architecture in Fig. 4a, $T(s)$ in (13) should be the transfer function from u_h to y_h including not only the actual robots but also the virtual robot. The transfer function $T(s)$ varies depending on the network and gain k . Although it also relies on a_{ij} , b_{ij} and the number of robots n , we fix them to $a_{ij} = b_{ij} = 1$ for all $(i, j) \in \mathcal{E}$ and $n = 10$ due to the space constraint. Here, we take the three different types of networks employed in the experimental section of Hatanaka et al. (2015a) as shown in Fig. 6a, and check the Nyquist plots for each network by changing k . Remark that the transfer function $(1/s)H(s)$ is confirmed to be Lyapunov stable in every case.

The plots for $k = 0.2$, 0.5 and 0.8 are shown in Figs. 6b–d, respectively. We see from these figures that the impact coefficient ϵ (minus of the smallest negative real part) is at most 0.2 for all networks when $k = 0.2$, it is at most 0.4 when $k = 0.5$ and hence Assumption 2 is satisfied for these k .

Fig. 7 Graph type used in simulation (left) and the nyquist plot of $(1/s)H_q(s)$ with $k = 0.9$ (right)



However, the assumption is violated in the case of $k = 0.8$ only for the network type 2.

It is also observed by comparing these figures that ϵ is monotonically increasing as k gets large. From (17), the gain k is regarded as a measure of the effects from the actual robotic swarm whose dynamics is more complicated than the virtual robot, a single integrator. The above results thus provide an insight that it is hard for an operator to attain passivity when he/she controls a complicated dynamical system. Conversely, choosing a small k renders the operator nearly passive. However, instead, information on the environment where the actual robots live is not vividly fed back to the human, which would degrade the human high-level decisions and recognitions originally expected for semi-autonomous systems. The above discussions suggest a fundamental trade-off between the human passivity and the performance of the high-level human tasks. An appropriate selection of k is an interesting subject but exceeds the scope of this specific paper. We thus leave the issue as a future work, and provide only a tentative conclusion that Assumption 2 is expected to hold as long as k would be appropriately selected.

Remark finally that, in the intended system, the human operator is MIMO with 2-dimensional input and output. Thus, precisely speaking, the above discussions on Nyquist plot may not be directly applied to the present case, but it would be applicable at least under the hypothesis that the human actions are almost decoupled between x - and y -coordinate.

6.2 Verification on synchronization

In this subsection, we verify the synchronization of the proposed architecture by using simulation for both position and velocity control mode. In the simulation we consider 5 robots in 1-D field with initial position $q_0 = [-2 \ 0 \ 1 \ 2 \ 5]^T$ m. The communication graph is a circle graph as shown in Fig. 7 (left) with two accessible robots. To run each simulation, we first have to prepare a model of the human operator.

Here, for the position control mode, we redefine the transfer function from u_h to y_h as $T_q(s)$ and the human

model as $H_q(s)$. Then, similarly with the previous subsection, we consider the model (13) which results in

$$H_q(s) = \frac{\omega_c}{sT_q(s)} e^{-\tau s} \tag{27}$$

with $\omega_c = 0.6$ rad/s, $\tau = 0.2$ s. The gain k is set as 0.9, and the Nyquist plot of the cascade system $(1/s)H_q(s)$ is shown in Fig. 7 (right) with impact coefficient $\epsilon = 0.423$. Thus, the Assumption 2 is satisfied for this k value.

Then, we set the reference position $r_q = 5$ m and run the simulation using the calculated $H_q(s)$. The movement of all robots and the corresponding velocities are shown in Fig. 8. It is observed that using this human model, all robots converge to r_q and it verifies the goal specified in (4).

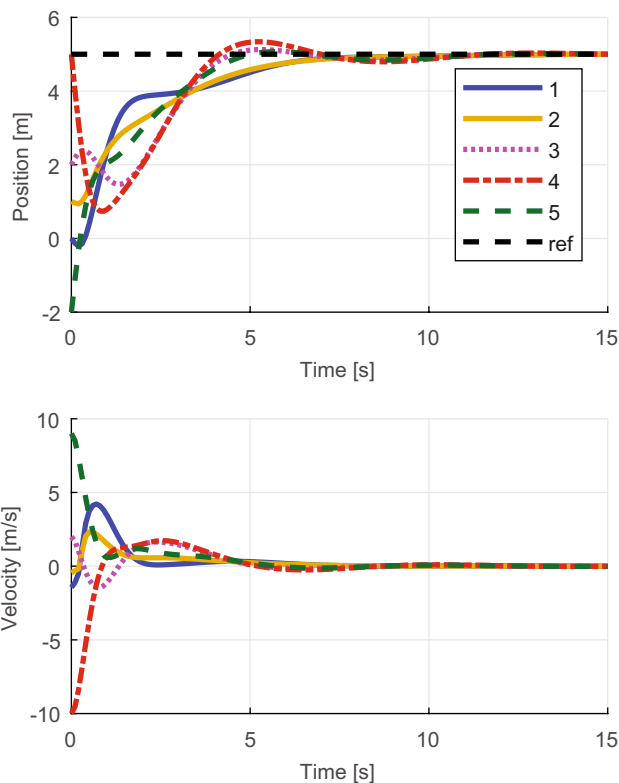


Fig. 8 Position control mode with reference position $r_q = 5$ m where all robots converge to r_q

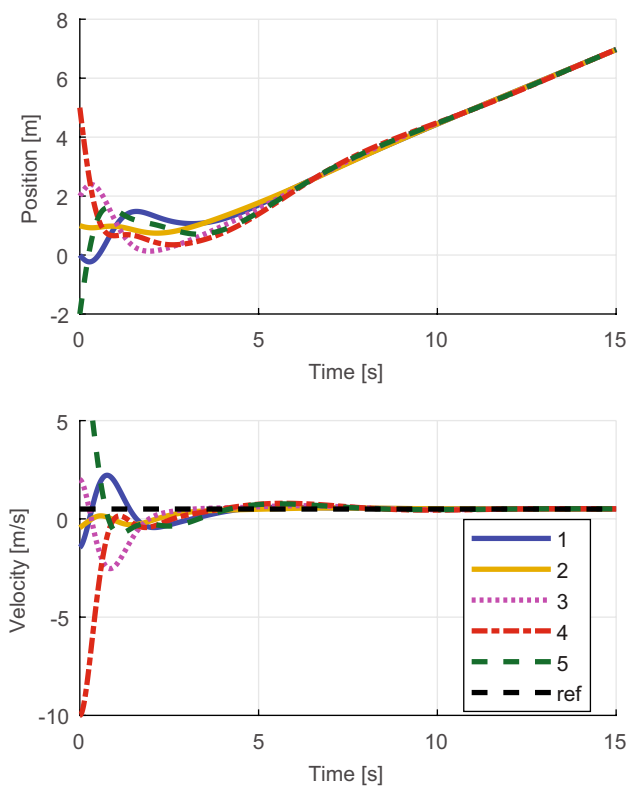


Fig. 9 Velocity control mode with reference velocity $r_v = 0.5$ m/s where all robots converge to the same position and move together with the same velocity r_v

Next, we continue with the simulation for velocity control mode. Here, we redefine the transfer function from u_h to y_h as $T_v(s)$ and the human model as $H_v(s)$. Note that by comparing y_h from the two modes in (17) and (20) it is easy to verify $T_v(s) = sT_q(s)$. Then, by using the same setup for the human model in (13) we obtain

$$H_v(s) = \frac{\omega_c}{sT_v(s)} e^{-\tau s} = \frac{\omega_c}{s^2 T_q(s)} e^{-\tau s}. \tag{28}$$

Differing from the position control mode, Assumption 3 only requires the impact coefficient of the human model $H_v(s)$. From (28), we have $H_v(s) = (1/s)H_q(s)$. Therefore, $H_v(s)$ has the same impact coefficient $\epsilon = 0.423$ and satisfies Assumption 3.

The velocity reference is set as $r_v = 0.5$ m/s and the results of the simulation using the calculated $H_v(s)$ are shown in Fig. 9. It is observed that all robots converge to the same position while moving together with the same velocity as r_v . Thus, we confirm that the goal in (5) is achieved.

To close the section, we would also like to point out that (Hatanaka et al. 2015a, 2017b) present a method to examine the human operator passivity through experiments on a human-in-the-loop simulator. After retrieving data from several trial subjects, techniques of closed-loop system identification is used to identify $H(s)$. The passivity property of the human operator is then discussed using bode diagram of $H(s)$. Note that the approach can also be used to investigate the passivity-short assumption in the current architecture, and we leave this issue as a future work.

7 Experimental verification

In this section, we show an implementation of our proposed architecture on a planar experimental testbed. Here, we demonstrate that the architecture works even with many disturbances, such as vehicle dynamics, imperfect actuation, friction wheels, and imperfect tracking of low-level controllers.

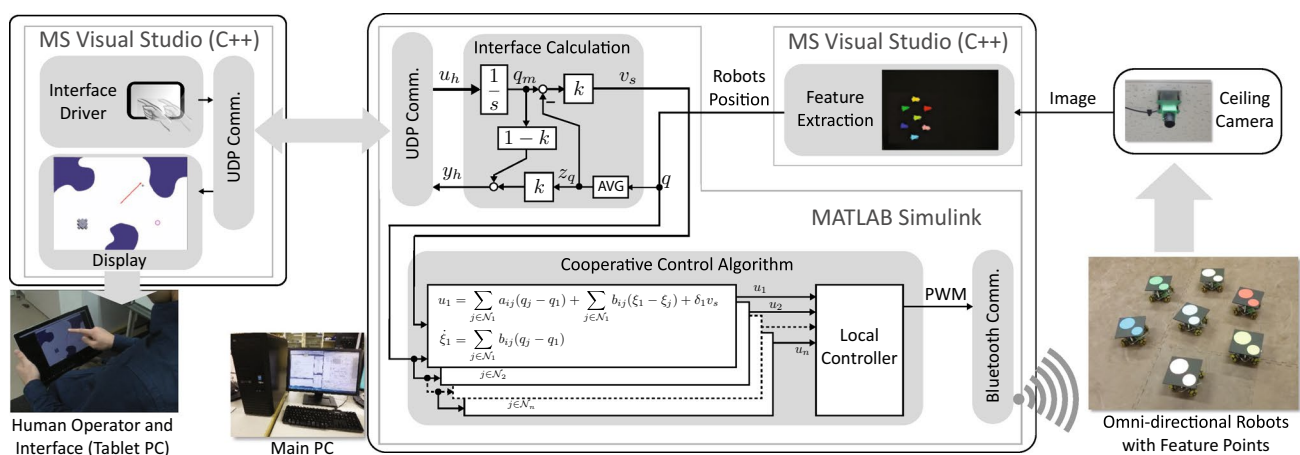


Fig. 10 Implementation setup for the testbed. The main PC calculates the feature extraction and the distributed operation of the proposed architecture. The human operator is holding a Tablet PC as an interface and communicate with the main PC through UDP communication

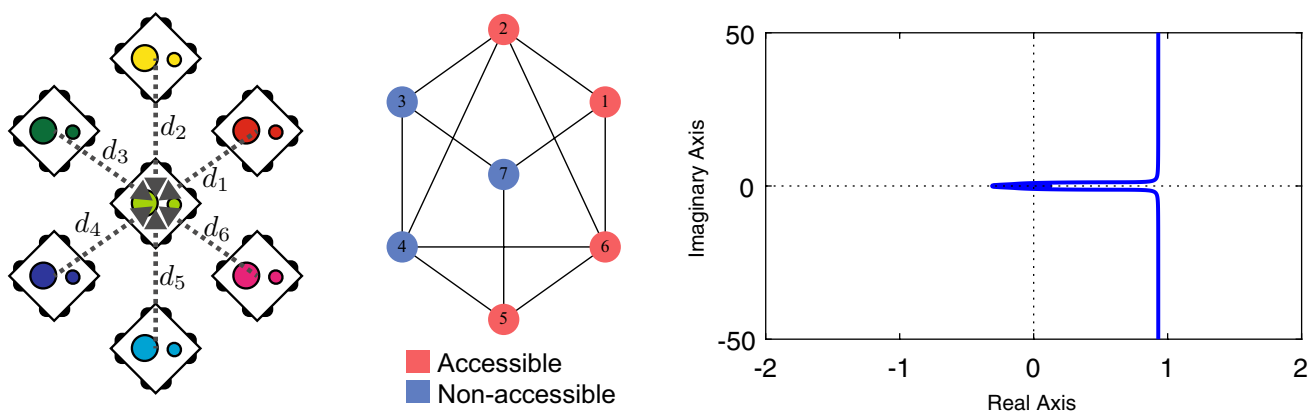


Fig. 11 Configuration of all the robots with bias (left), communication graph (middle) and nyquist plot of $(1/s)H(s)$ for the given setup with $k = 0.8$ (right)

Table 1 Biases for all robots

| | d_1 | d_2 | d_3 | d_4 | d_5 | d_6 | d_7 |
|-------|-------|-------|-------|-------|-------|-------|-------|
| x (m) | -0.28 | 0 | 0.28 | 0.28 | 0 | -0.28 | 0 |
| y (m) | -0.2 | -0.4 | -0.2 | 0.2 | 0.4 | 0.2 | 0 |

7.1 Experiment setup

The experiment setup is illustrated in Fig. 10. It is based on Hatanaka et al. (2017a) with an additional calculation of the passivity-short interconnection. Here, we use seven omnidirectional robots TDO48 (Tosadenshi Ltd.) with a maximum speed of 0.5 m/s. Feature points are attached on top of each robot, and a ceiling camera Firefly MV (PointGray) captures images of all robots on the field. Then, the positions of all robots are obtained by using a feature extraction algorithm with library OpenCV 2.0 in Microsoft Visual Studio.

The interface calculation and the cooperative control algorithm in the proposed architecture are implemented on Simulink. Additionally, local controllers are also added in Simulink to ensure that the dynamics of each robot is close to an integrator. Each local controller interprets each velocity input signal to a PWM value. This PWM value is then sent to each robot via Bluetooth communication. Both the feature extraction algorithm and the Simulink calculation are run on a PC with Core i7, CPU 3.4 GHz, and 8 GB RAM. Note that while it is technically possible to implement the system in a real distributive manner, the current setup eases the communication between each calculation part.

On the human operator side, a tablet PC (Surface Pro 4) runs a program (in Microsoft Visual Studio) that displays the visual information y_h and reads the touchscreen input

for the human command u_h . These interface signals u_h and y_h are exchanged through UDP communication between main PC and the tablet PC.

To avoid collisions at the final configuration, we select the biases $d_i, i = \{1, \dots, 7\}$ as shown in Table 1 and illustrated in Fig. 11 (left). The communication graph in the experiment is shown in Fig. 11 (middle) with the communication gain $a_{ij} = 0.2$ and $b_{ij} = 0.05$. The accessible robots are $\mathcal{V}_h = \{1, 2, 5, 6\}$, and the gain k is set to be 0.8. Based on this setup, we approximate the model of the human operator using (13) and plot the $(1/s)H(s)$ in Fig. 11 (right) which yields an impact coefficient of 0.308. Thus, it is expected that the human operator fulfills Assumption 2.

7.2 Scenario and results

In the experiment scenario, the human operator is asked to navigate the robots to the reference position with the presence of obstacles. Through the interface, the human operator receives the visual feedback y_h , the information of obstacles and also the reference position r_q . Then, by providing the human command u_h through the touchscreen, the human operator navigates the y_h to r_q while avoiding the obstacle. Since each robot is not equipped with any obstacle avoidance algorithm, it is expected that the human operator manages to navigate based on the presented information in the interface.

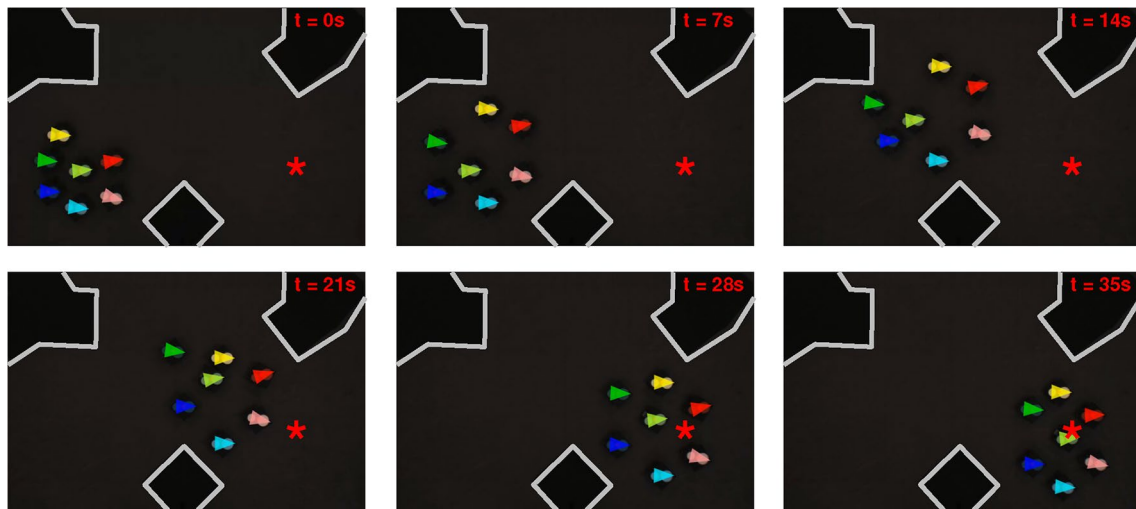


Fig. 12 Snapshots of the robots' movement in the experiment for position control mode and obstacle avoidance. The reference position r_q is shown as star and the boundary of the obstacles are shown as

gray lines. The human operator manages to navigate all robots to the reference position even with the presence of obstacles

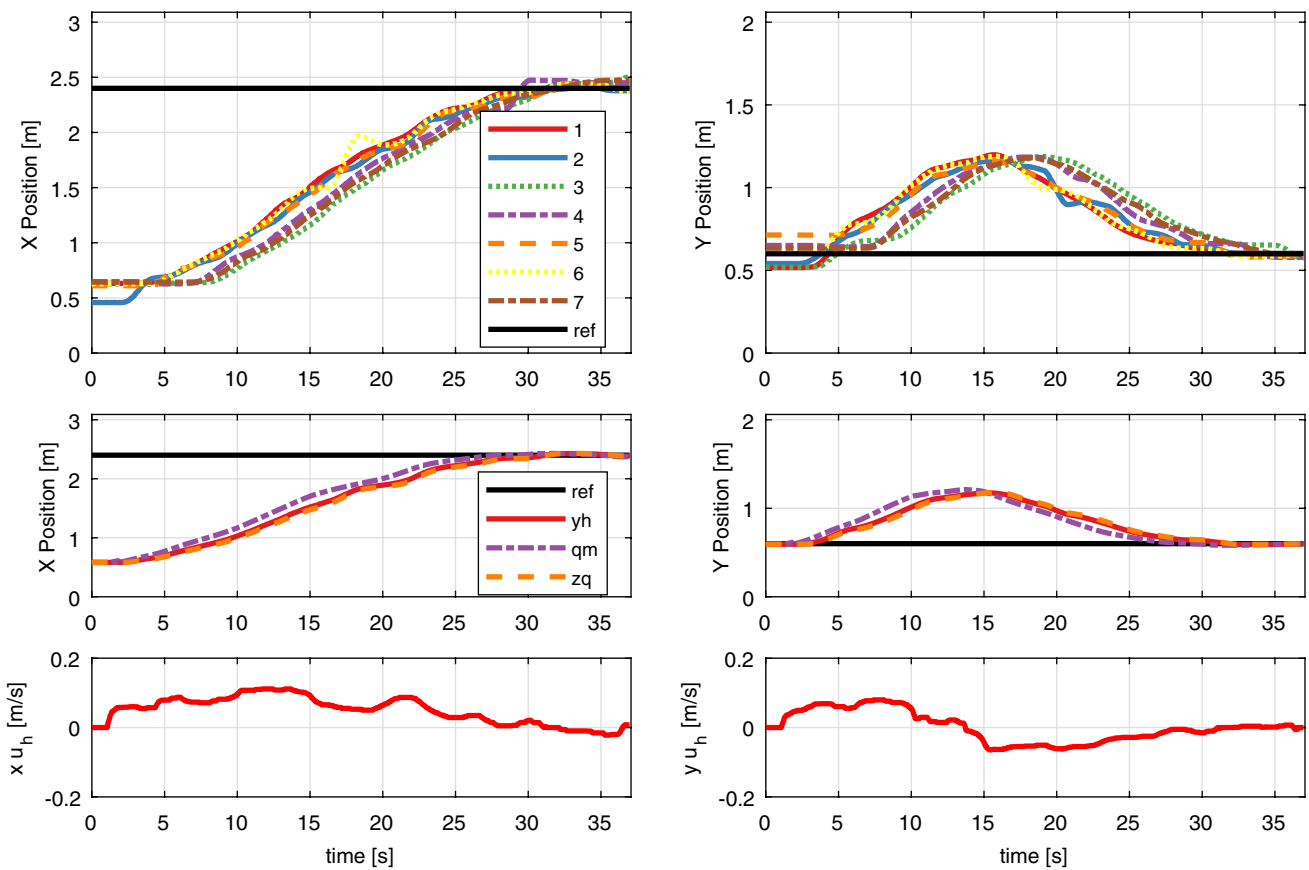


Fig. 13 Time responses of the position with bias (top), the interface signals (middle) and human command u_h (bottom) in both x and y dimensions. The biased positions of the robots converge to the reference position

The snapshots of the experiment are shown in Fig. 12 where the human operator manages to navigate all robots to the reference position. Figure 13 presents the time response of the biased positions, interface signals, and the human command. As the biased positions converge to the reference position, all robots result in the intended formation. Thus, we confirm the position synchronization of the robotic swarm to human's reference.

Remark that by providing only a single visual feedback y_h , the cognitive burden of the human operator is reduced because he does not have to control each robot individually. It also implies the separation of the high-level navigation task to the human operator and the low-level synchronization to the architecture. In addition, by inspecting the interface signals in Fig. 13 we can observe that with the current $k = 0.8$ the visual feedback y_h closely represents the average position of the accessible robot z_q . This aids the human operator to complete the experiment scenario by providing vivid visual information of the accessible robots.

8 Conclusion

In this paper, we presented an approach to distributed control of the semi-autonomous robotic swarm. The control goal is set to synchronization of all robot positions or velocities to a reference value desired by the human operator. The architecture interconnecting the human operator and the robotic swarm is constructed based on positive feedback interconnections of passivity-short systems. By assuming human operator's thought process as a passivity-short system, we proved the position and velocity synchronization. Then, we presented a model based discussion with simulation results to verify the assumption on the human operator and the achievement of the control goals. Finally, we demonstrated the architecture on an experimental testbed where the human operator manages to navigate all robots to the reference position even with the presence of obstacles.

Acknowledgements We acknowledge the financial support from JSPS KAKENHI Grant Nos. 15H04019 and 18H01459.

References

Atashzar, S.F., Shahbazi, M., Tavakoli, M., Patel, R.V.: A passivity-based approach for stable patient–robot interaction in haptics-enabled rehabilitation systems: modulated time-domain passivity control. *IEEE Trans. Control Syst. Technol.* **25–3**, 991–1006 (2017)

Bai, H., Freeman, R.A., Lynch, K.M.: Robust dynamic average consensus of time-varying inputs. In: 49th IEEE Conf. decision and control, pp. 3104–3109 (2010)

Colgate, J.E.: Coordinate transformations and logical operations for minimizing conservativeness in coupled stability criteria. *Trans. ASME J. Dyn. Syst. Meas. Control* **116–4**, 643–649 (1994)

Cummings, M.L.: Human supervisory control of swarming networks. In: 2nd annual swarming: autonomous intelligent networked system conference, pp. 1–9 (2004)

Dyck, M., Zajayeri, A., Tavakoli, M.: Is the human operator in a teleoperation system passive? In: 2013 world haptics conf., pp. 683–688 (2013)

Egerstedt, M.: Human interactions with complex networks. In: Samad T, Annaswamy AM (eds.) *The impact of control technology*, 2nd edition, IEEE Control Systems Society. <http://www.ieeecs.org> (2014). Accessed 10 Oct 2017

Franchi, A., Secchi, C., Son, H.I., Bulthoff, H.H., Giordano, P.R.: Bilateral teleoperation of groups of mobile robots with time-varying topology. *IEEE Trans. Robot.* **28–5**, 1019–1033 (2012a)

Franchi, A., Secchi, C., Ryll, M., Bulthoff, H.H., Giordano, P.R.: Shared control: balancing autonomy and human assistance with a group of quadrotor UAVs. *IEEE Robot. Autom. Mag.* **19–3**, 57–68 (2012b)

Freeman, R.A., Yang, P., Lynch, K.M.: Stability and convergence properties of dynamic average consensus estimators. In: 45th IEEE conf. decision and control, pp. 338–343 (2006)

Giordano, P.R., Franchi, A., Secchi, C., Bulthoff, H.H.: A passivity-based decentralized strategy for generalized connectivity maintenance. *Int. J. Robot. Res.* **32–3**, 299–323 (2013)

Hatanaka, T., Chopra, N., Fujita, M.: Passivity-based bilateral human-swarm-interactions for cooperative robotic networks and human passivity analysis. In: 54th IEEE Conf. decision and control, pp. 1033–1039 (2015a)

Hatanaka, T., Chopra, N., Fujita, M., Spong, M.W.: *Passivity-based Control and Estimation in Networked Robotics*. Springer, Switzerland (2015b)

Hatanaka, T., Chopra, N., Yamauchi, J., Doi, M., Kawai, Y., Fujita, M.: A passivity-based system design of semi-autonomous cooperative robotic swarm. *ASME DSC Mag.* **139–6**, 14–18 (2017a)

Hatanaka, T., Chopra, N., Yamauchi, J., Fujita, M.: A passivity-based approach to human-swarm collaborations and passivity analysis of human operators. In: Wang, Y., Zhang, F. (eds.) *Trends in Control and Decision-Making for Human–Robot Collaboration Systems*, pp. 325–355. Springer, Switzerland (2017b)

Hirche, S., Buss, M.: Human-oriented control for haptic teleoperation. *Proc. IEEE* **100–3**, 623–647 (2012)

Hokayem, P.F., Spong, M.W.: Bilateral teleoperation: an historical survey. *Automatica* **42–12**, 2035–2057 (2006)

Kolling, A., Walker, P., Chakraborty, N., Sycara, K., Lewis, M.: Human interaction with robot swarms: a survey. *IEEE Trans. Hum. Mach. Syst.* **46–1**, 9–26 (2016)

Lee, D., Spong, M.W.: Bilateral teleoperation of multiple cooperative robots over delayed communication networks: theory. In: *Proc. IEEE Int. Conf. Robotics and Automation*, pp. 360–365 (2005)

Lee, D., Franchi, A., Son, H.I., Ha, C., Bulthoff, H.H., Giordano, P.R.: Semiautonomous haptic teleoperation control architecture of multiple unmanned aerial vehicles. *IEEE/ASME Trans. Mechatron.* **18–4**, 1334–1345 (2013)

Liu, Y.C., Chopra, N.: Controlled synchronization of heterogeneous robotic manipulators in the task space. *IEEE Trans. Robot.* **28–1**, 268–275 (2012)

McLurkin, J., Smith, J., Frankel, J., Sotkowitz, D., Blau, D., Schmidt, B.: Speaking swarmish: Human-robot interface design for large swarms of autonomous mobile robots. In: *AAAI spring symposium*, pp. 72–76 (2006)

- McRuer, D.: Human dynamics in man-machine systems. *Automatica* **16–3**, 237–253 (1980)
- Mekdeci, B., Cummings, M.L.: Modeling multiple human operators in the supervisory control of heterogeneous unmanned vehicles. In: *Proc. 9th workshop on performance metrics for intelligent systems*, pp. 1–8 (2009)
- Music, S., Hirche, S.: Control sharing in human–robot team interaction. *Annu. Rev. Control* **44**, 342–354 (2017)
- Nuno, E., Basanez, L., Ortega, R.: Passivity-based control for bilateral teleoperation: a tutorial. *Automatica* **47**, 485–495 (2011)
- Olsen, D.R., Wood, B.: Fan-out: Measuring human control of multiple robots. In: *Proc. SIGHCI Conf. human factors in computing systems*, pp. 231–238 (2004)
- Qu, Z.: An impact equivalence principle of separating control designs for networked heterogeneous affine systems. *IFAC Proc. Vol.* **45–26**, 210–215 (2012)
- Qu, Z., Simaan, M.A.: Modularized design for cooperative control and plug-and-play operation of networked heterogeneous systems. *Automatica* **50–9**, 2405–2414 (2014)
- Rodriguez-Seda, E.J., Troy, J.J., Erignac, C.A., Murray, P., Stipanovic, D.M., Spong, M.W.: Bilateral teleoperation of multiple mobile agents: coordinated motion and collision avoidance. *IEEE Trans. Control Syst. Technol.* **18–4**, 984–992 (2010)
- Secchi, C., Franchi, A., Bulthoff, H.H., Giordano, P.R.: Bilateral teleoperation of a group of UAVs with communication delays and switching topology. In: *Proc. IEEE Int. conf. robotics and automation*, pp. 4307–4314 (2012)
- Stipanovic, D.M., Hokayem, P.F., Spong, M.W., Siljak, D.D.: Cooperative avoidance control for multiagent systems. *Trans. ASME J. Dyn. Syst. Meas. Control* **129–5**, 699–707 (2007)
- Wang, X., Wang, Y.: Co-design of control and scheduling for human-swarm collaboration systems based on mutual trust. In: Wang, Y., Zhang, F. (eds.) *Trends in Control and Decision-Making for Human-Robot Collaboration Systems*, pp. 387–413. Springer, Switzerland (2017)
- Xia, M., Rahnama, A., Wang, S., Antsaklis, P.J.: On guaranteeing passivity and performance with a human controller. In: *2015 23th Mediterranean conf. control and automation*, pp. 722–727 (2015)
- Yun X., Yamamoto, Y.: Internal dynamics of a wheeled mobile robot. In: *Proc. 1993 IEEE/RSJ Int. conf. intelligent robots and systems*, pp. 1288–1294 (1993)
- Wang, Y., Zhang, F. (eds.): *Trends in Control and Decision-Making for Human–Robot Collaboration Systems*. Springer, Switzerland (2017)



Made Widhi Surya Atman received his B.Eng. and M.Sc. degrees in electrical engineering from Institut Teknologi Bandung, in 2011 and 2014. In 2017, he received M.Eng. degrees in Mechanical and Control Engineering from Tokyo Institute of Technology. Currently, he is a doctoral student at Department of Systems and Control Engineering, Tokyo Institute of Technology. His current research interests include human–robotic swarm interaction and passivity-based control.



Takeshi Hatanaka received the Ph.D. degree in applied mathematics and physics from Kyoto University in 2007. He then joined Tokyo Institute of Technology in 2007, where he held positions as an assistant and associate professor. In 2016, he spent an eight-month sabbatical at School of Engineering and Applied Sciences of Harvard University. Since April 2018, he is an associate professor at Osaka University. He is the coauthor of *Passivity-Based Control and Estimation in Networked Robotics* (Springer, 2015). His research interests include networked robotics and energy management systems. He received the Kimura Award (2017), Pioneer Award (2014), Outstanding Book Award (2016) and Outstanding Paper Awards (2009, 2015) all from SICE. He also received 10th Asian Control Conference Best Paper Prize Award (2015). He is an AE for IEEE TSCT and SICE JCMSI, and a member of the Conference Editorial Board of IEEE CSS.

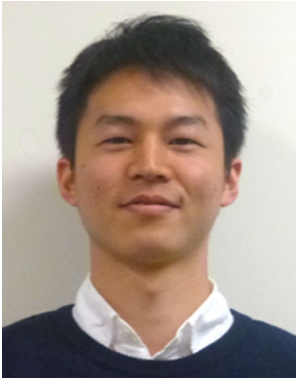


Zhihua Qu received the Ph.D. degree in electrical engineering from the Georgia Institute of Technology, Atlanta, in June 1990. Since then, he has been with the University of Central Florida (UCF), Orlando. Currently, he is the SAIC Endowed Professor in College of Engineering and Computer Science, a Pegasus Professor and the Chair of Electrical and Computer Engineering, and the Director of FEEDER Center. His areas of expertise are nonlinear systems and control, with applications to autonomous systems and energy/power systems. His recent work focuses upon control, optimization and plug-and-play operation of networked systems.



Nikhil Chopra is an Associate Professor in the Department of Mechanical Engineering at the University of Maryland, College Park. Prior to joining the University of Maryland, he was a Postdoctoral Research Associate in the Coordinated Science Laboratory at the University of Illinois at Urbana-Champaign from 2006–2007. He received a Bachelor of Technology (Honors) degree in Mechanical Engineering from the Indian Institute of Technology, Kharagpur, India, in 2001, M.S. degree in General Engineering in 2003, and his Ph.D. degree in Systems and Entrepreneurial Engineering in 2006 from the University of Illinois at Urbana-Champaign. His research interests include security and resilience of networked systems, control of networked autonomous systems, control

of mixed human-robot teams and co-design in complex systems. He is the co-author of the book *Passivity-Based Control and Estimation in Networked Robotics*. He is currently an Associate Editor of *IEEE Transactions on Control of Network Systems* and was previously an Associate Editor for *IEEE Transactions on Automatic Control*.



Junya Yamauchi received B.Eng. degree from Nagoya University, M. Eng. degree and Ph.D. degree from Tokyo Institute of Technology in 2013, 2015 and 2018, respectively. He is currently an Assistant Professor in the Department of Systems and Control Engineering, Tokyo Institute of Technology. His research interests include cooperative control of human-robotic networks, vision-based estimation and control.

"*Passivity-Based Control and Estimation in Networked Robotics*" (Springer, 2015). He was the CSS Vice President Conference Activities and a member of CSS Board of Governors. He served as the General Chair of the 2010 IEEE Multi-conference on Systems and Control. He was also the Head of SICE Technical Division on Control, the Chair of SICE Technical Committee on Control Theory and a Director of SICE. He served as an Associate Editor for the *IEEE Transactions on Automatic Control*, the *IEEE Transactions on Control Systems Technology*, *Automatica*, *Asian Journal of Control*, and an Editor for the *SICE Journal of Control, Measurement, and System Integration*. He is a recipient of the 2008 IEEE Transactions on Control Systems Technology Outstanding Paper Award, is a Plenary Lecturer of 54th IEEE Conference on Decision and Control in 2015, and is an IEEE Control System Society Distinguished Lecturer from 2017. He also received the 2010 SICE Education Award and the Outstanding Paper Awards from the SICE and ISCIE. He is a Fellow of IEEE and SICE.



Masayuki Fujita is a Professor at Tokyo Institute of Technology. He is also a Research Supervisor for Japan Science and Technology Agency (JST) Core Research for Evolutional Science and Technology (CREST). He received the Dr. of Eng. degree in Electrical Engineering from Waseda University, Tokyo, in 1987. Prior to his appointment at Tokyo Institute of Technology, he held faculty appointments at Kanazawa University and Japan Advanced Institute of Science and Technology. His research

interests include passivity-based control in robotics, distributed energy management systems and robust control. He is the coauthor of the book